Processing and Application of Ceramics 19 [1] (2025) 42–49
https://doi.org/10.2298/PAC2501042K

Behaviour of reactively sintered TiB_2-SiC composites under sudden impact

Dawid Kozień[1,*], Wojciech Banaś[1], Stanisław Cudziło[2], Adrian Graboś[3], Katarzyna Pasiut[1], Waldemar Pyda[1], Agnieszka Wojteczko[1], Marek Grabowy[4], Zbigniew Pędzich[1]

[1] *Department of Ceramics and Refractories, Faculty of Materials Science and Ceramics, AGH University of Krakow, Al. Mickiewicza 30., 30-059 Krakow, Poland*
[2] *Faculty of Advanced Technologies and Chemistry, Military University of Technology, 2 Ul. Gen. Sylwestra Kaliskiego 2, 00-908 Warsaw, Poland*
[3] *Tohoku University, Tohoku Forum for Creativity, 2-1-1 Katahira, Aoba-ku, Sendai 980-8577, Japan*
[4] *Institute of Power Engineering, Ceramic Branch CEREL, 1 Techniczna St., 36-040, Boguchwała, Poland*

Received 3 March 2024; Received in revised form 23 January 2025; Accepted 22 February 2025

Abstract

With each passing year, multi-layered armours for military vehicles become more and more advanced to meet growing demands and counterpart novel offensive solutions. Layers that are responsible for track deviation and blunting of the projectile, typically made of hard ceramics, are nowadays considered to be replaced by ceramic composite. In this study, two ceramic systems composed of the TiB_2 *matrix and SiC or SiC/TiC reinforcement phases were fabricated from mixture of* B_4C *powder with different amount of* $TiSi_2$ *or* Ti_5Si_3 *intermetallic phases. Importantly, the desirable microstructure was obtained by reactive sintering at 1550 °C and pressure of 2.5 GPa. The obtained ceramic composites underwent dynamic loading tests to evaluate their applicability for ballistic shields. Two systems were then compared in terms of the potential pulverization rate which determines usability as a primary layer for a multi-layered vehicle armour.*

Keywords: *boron carbide, titanium silicide* $TiSi_2$*, titanium silicide* Ti_5Si_3*, composites, armour*

I. Introduction

Currently, the demand for improvement of military technology is an especially important topic. Many countries increase their spending expenditure according to the regional geopolitical occurrences of the last decade.

Armoured vehicles warfare remains one of the crucial aspects within the modern battlefield concept. To that end, there is a constant competition to develop highly resilient, often reactive armour that is as lightweight as possible. Materials which have low density allow greater mobility. Ballistic resistance is one more crucial factor in armour, traditionally linked to hardness and Young's modulus. Recent studies by Woodward [1] and Krell and Strassburger [2] showed that dynamic compressive strength also plays a significant role in ballistic resistance. Therefore, enhancing ballistic resistance is a key for developing effective armour layers' materials. With that in mind, ceramic composites are materials well-suited to meet the needs of modern battlefields [3,4]. They could potentially replace traditional hard ceramics as layers responsible for the projectile or shrapnel track deviation, blunting and overall absorption of their energy. Still, they require pioneering research efforts.

There are various scientific paths taken to achieve the described goals in armours materials. One promising research direction is the composite synthesis employing high-purity ceramics [5] to create materials with low density, high hardness and high dynamic compressive strength. Another solution is the fabrication of multilayer composite armours using polyesters and natural fibres [6], and multilayer metal/UHMWPE/SiC composites [4]. A considerable number of studies have

---

[*] Corresponding author: +48 798 860 526
e-mail: *kozien@agh.edu.pl*

been conducted on free ceramic particle armour (FCPA) [7]. There are also well documented concepts of alumina microbeads [8] and shear thickening fluids (STFs) [9,10] as ceramic-polymer composites to be used as an armour. Lastly, advanced ceramic composites obtained by novel or repeatedly emerging methods, such as spark plasma sintering (SPS), that contain classic ballistic ceramics (e.g. SiC, Al_2O_3 or B_4C) show great overall potential [11,12]. The latter topic is within interest of the studies conducted by our group.

Boron carbide is characterized by low density (theoretical density of 2.52 g/cm^3) [13–15], high hardness (over 30 GPa) [14,16], excellent mechanical properties [14], inertness to acids [14,16,17] and high melting point [16,18]. Owing to its unusual structure, it is possible to obtain boron carbides with different stoichiometry [13]: carbon-rich boron carbide [19] and boron-rich boron carbide [18,20,21]. In these researches, B_4C was usually combined with carbon and polymers to produce material systems of very low density, allowing for extremely high weight reduction, while maintaining sufficient volume. However, the proposed solution has its downsides. Polymer compounds have low thermal resistance (decomposing at temperatures of ~100 °C) and the lowest mechanical properties of all engineering materials. This may lead to problematic issues at the stage of further mechanical engineering regarding combat armour vehicles. Ideally, a more property coherent system should be developed.

Nowadays, more and more research on TiB_2-SiC composites is being conducted due to a wide range of applications for such materials. There is also great potential for their modifications and development of various methods to obtain them. A popular way to produce SiC-TiB_2 composites is their sintering from a mixture of B_4C and Ti-Si intermetallic phases. Wang *et al.* [22] and Wang *et al.* [23] demonstrated the feasibility of fabricated B_4C-SiC-TiB_2 composites characterized by exceptionally high hardness, i.e. a crucial parameter for this particular part of military vehicle armour. They earned a name "super-hard" [22]. These results [23] sparked a discussion of the possibility of preparing materials with high relative porosity using a relatively low sintering temperature. The "super-hard" properties of B_4C-TiB_2-SiC composites were also noted by Rodríguez-Rojas *et al.* [24]. The composite obtained from B_4C, α-SiC and TiB_2 precursor powders showed high hardness reaching up to 35 GPa [24], even higher than the one achieved by Wang *et al.* (30 GPa) [22]. Other studies considered their use as an infrared source material for example [25].

In general, composites have better properties than the usual constituent compounds. The research on the properties of SiC-TiB_2 composites obtained by SPS proved these compounds to exhibit better properties than the pure SiC, e.g. better fracture toughness, an improvement which is the second key parameter in ceramic composites [26]. Investigations were also carried out to prepare SiC-TiB_2 composites for protective applications, using B_4C, Ti_3SiC_2 and Si as precursors. The results demonstrated some ability of the composites to protect light military vehicles [27].

The main goal of our study was to obtain and evaluate a TiB_2-based ceramic composite material for potential use in military vehicle armours. The material resulted from reactive sintering of B_4C and stoichiometric amounts of $TiSi_2$ or Ti_5Si_3 intermetallic phases. The obtained material systems were subjected to a series of tests to determine basic material properties. Additionally, scanning electron microscopy (SEM) and powder X-ray diffraction (XRD) were used to evaluate microstructural features of the materials. Subsequently, a dynamic loading test and a comparison of potential pulverization rates of the obtained ceramic composites were done to assess their potential usability as military vehicle armours.

II. Experimental

The initial materials used in the composites preparation were commercial B_4C powder (99% purity, Grade HD 07, H.C. Starck), carbon black (Tujmazy P-803) and $TiSi_2$ or Ti_5Si_3 powders produced via the method based on the self-propagating, high-temperature synthesis (SHS) process elaborated by Chlubny *et al.* [28]. The mass proportions of the individual compounds were determined, considering the purity of the commercial B_4C powder and the composition of the stoichiometric system (referred in the abstract and further in the manuscript as systems of "stoichiometric amounts"). The molar masses of the precursors were measured, using the following reactions:

$$2\,TiSi_2 + B_4C + 3\,C \longrightarrow 2\,TiB_2 + 4\,SiC \tag{1}$$

$$2\,Ti_5Si_3 + 5\,B_4C + C \longrightarrow 10\,TiB_2 + 6\,SiC \tag{2}$$

Additionally, the composition containing 20 wt.% of intermetallic compounds was created for the flat amount reference. All the sample compositions are given in Table 1.

The green powder mixtures with the respective proportions were pressed on a uniaxial bi-directional press to form cuboidal lozenges with a hexagonal base, each with a mass of 30 g. Subsequently, the samples were sintered under high-pressure and high-temperature conditions (HP-HT sintering) at 1550 °C and pressure of 2.5 GPa in an inert atmosphere for 2 h. After sintering,

Table 1. Composition of raw compounds used for preparation of composites

Sample	Composition [wt.%]			
	B_4C	$TiSi_2$	Ti_5Si_3	Carbon black
$B_4C/TiSi_2$-S	18.306	69.635	-	12.069
$B_4C/TiSi_2$-20	80.000	20.000	-	-
B_4C/Ti_5Si_3-S	29.323	-	69.389	1.228
B_4C/Ti_5Si_3-20	80.000	-	20.000	-

the porosity, water absorption and density were measured using a hydrostatic method. Additionally, the final microstructures were evaluated with X-ray diffraction (XRD) and scanning electron microscopy coupled with energy dispersive X-ray spectroscopy (SEM + EDS). X-ray diffraction analysis of the stoichiometric samples was performed using Cu-lamp diffractometer, Johansson monochromator, and X'Celerator strip detector. The test materials were treated in a mortar and then placed in a cuvette for the XRD measurements. A single test was carried out over the 5–90° range with a step of 0.01° and a total measurement time of 4 h. The microstructures of the stoichiometric composite samples were observed with an ultra-high-resolution scanning electron microscope with a field emission gun (FEG-Schottky emitter) - NOVA NANO SEM 200 (FEI Europe Company) in cooperation with an EDS analyser (EDAX). Prior to the observations, a thin layer of gold was deposited on the samples surface. The tests were carried out under high vacuum conditions ($< 10^{-2}$ Pa), an accelerating voltage of 18 kV and a resolving capacity of up to 2 nm.

To determine usability of the obtained ceramic composites as vehicle armour, the dynamic-load test was performed (Fig. 1). The plates were loaded with an electric detonator containing 190 ± 10 mg of an explosive material pressed into a dural shell of a 6.2 mm inner diameter and 0.5 mm wall thickness. The detonator height was 17.0 mm, excluding the electrical wires. During the tests, the plate with the attached detonator was placed in the explosive chamber so as to collect the maximal amount of debris after the detonation. Due to the military confidentiality other information regarding the dynamic load test conducted at Military University of Technology cannot be stated.

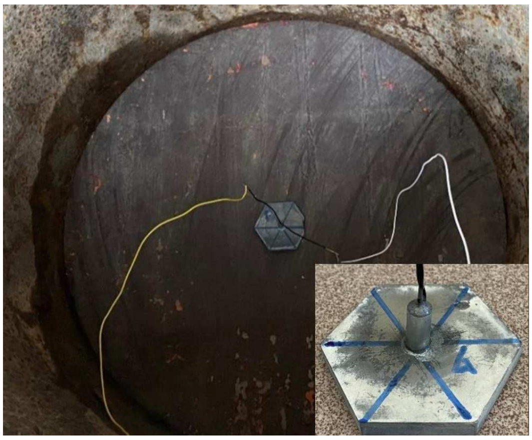

Figure 1. Photographs of the sample with a detonator placed in an explosive chamber and of the sample with an attached explosive charge (inset)

III. Results and discussion

3.1. Phase composition of the synthesized powders

X-ray diffraction analysis of the synthesized $TiSi_2$ and Ti_5Si_3 intermetallic powders was carried out and results are shown Figs. 2 and 3. The XRD patterns indicated the purity of the applied intermetallic compounds, which was consistent with the results of Chlubny's study [28].

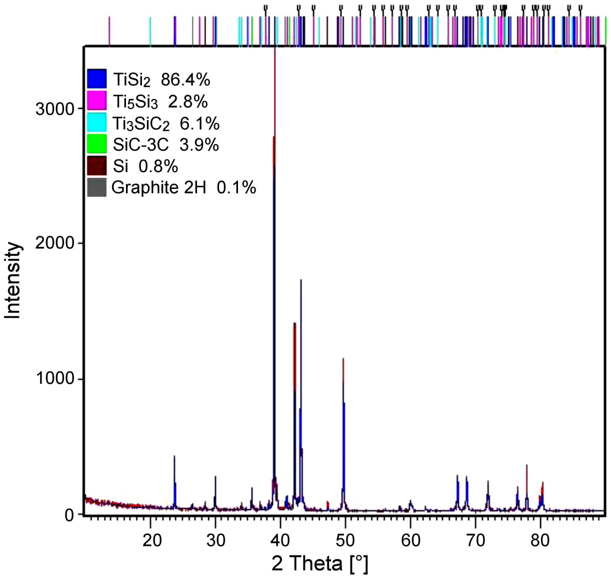

Figure 2. XRD diffraction pattern of the obtained $TiSi_2$ powder

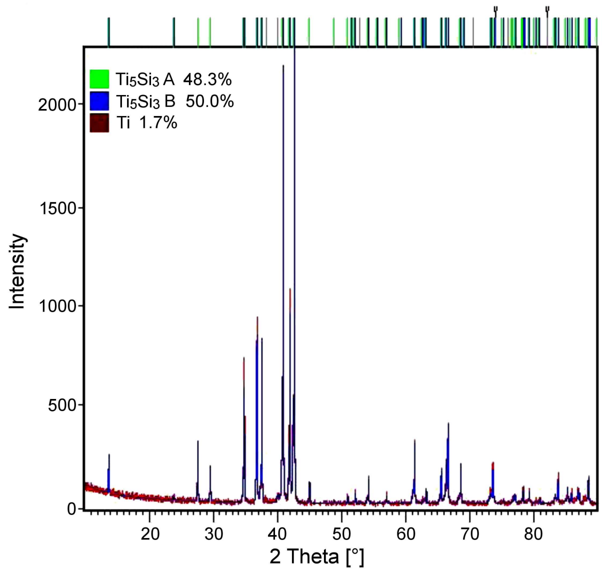

Figure 3. XRD diffraction patterns of the obtained Ti_5Si_3 powder

3.2. Density and porosity of the sintered samples

The measured values of density and porosity of the sintered ceramic composites are presented in Table 2. Based on the results, it can be determined that the elementary properties (open porosity and density) increased directly in relation to the mass of intermetallic compounds used as precursors. Notably, there was a significant difference depending on the type of intermetallic phase. A higher increase in values was observed for the Ti_5Si_3 additive than for the same mass proportion of the $TiSi_2$ intermetallic precursor.

Table 2. Open porosity and density of the sintered samples

Sample	Open porosity [%]	Density [g/cm^3]
$B_4C/TiSi_2$-S	33.08	2.593
$B_4C/TiSi_2$-20	25.59	2.506
B_4C/Ti_5Si_3-S	35.92	2.697
B_4C/Ti_5Si_3-20	2.06	2.574

3.3. XRD analyses of the sintered samples

The results revealed in the XRD diffraction pattern (Fig. 4a) indicated that the stoichiometric sample with $TiSi_2$ phase ($B_4C/TiSi_2$-S) consisted of three phases: TiB_2, SiC-3C and $TiSi_2$. The presence of the first two phases was theoretically foreseen before the material was obtained, but the unreacted $TiSi_2$ phase indicates incomplete sintering. The XRD pattern of the B_4C/Ti_5Si_3-S sample with a stoichiometric precursor ratio (Fig. 4b) indicated the presence of four phases. The presence of TiB_2 and SiC-3C phases was theoretically predicted, and the formation of TiC resulted from the reaction of carbon (including B_4C) with titanium from the precursor powders. The similar process was observed in the previous study [28].

The diffractograms also showed that the $TiSi_2$ (Fig. 4a), and Ti_5Si_3 (Fig. 4b) intermetallic phases were insufficiently sintered within their respective systems, which calls for further optimization of the process parameters.

3.4. SEM/EDS analyses of the sintered samples

The SEM observations of the sintered sample derived from stoichiometric proportions of B_4C-$TiSi_2$ precursor mixture are shown in Fig. 5 with respective EDS determined at three selected points. A superfused silicon carbide (SiC) phase and the usual SiC phase were identified at the point 1 and 2, respectively. Point 3 marks the area where two carbide phases were present: titanium carbide (TiC) and silicon carbide (SiC) and further observations revealed the presence of the TiB_2 phase too.

SEM analysis with respective EDS of the sintered sample $B_4C/TiSi_2$-S derived from the stoichiometric B_4C-Ti_5Si_3 precursor mixture (Fig. 6) revealed the presence of three main phases. Point 1 represented the titanium carbide (TiC) phase. Point 2 included an area of titanium boride (TiB_2) and traces of the unreacted Ti_5Si_3. Titanium boride took the form of bright, finely elongated rods. The TiB_2 presence was predicted in theoretical calculations when creating compositions for pressing and sintering. Point 3 marked an area consisting mainly of titanium boride (TiB_2), but also with traces of other compounds. The presence of all the compounds at each point was also confirmed by the previous XRD analysis.

Two samples of the stoichiometric amounts showed similar microstructural features (Figs. 5 and 6). The matrix was formed by boride compounds, whiles the carbide-based reinforcement and small amounts of intermetallic phases, leftovers of insufficient sintering, were observed as common irregularities. In both systems the composite phases were clearly distinguished and the boundaries between them were long enough for the energy absorption during the impact. Such a microstructure, albeit its stated defects, made the systems derived from reactive sintering of stoichiometric amounts of precursors perform much better than the flat-amount samples containing 20% of intermetallic phase. Similar calculations and accordingly performed synthesis would be required to obtain such a specific microstructure. With that being said, the observed irregularities had detrimental overall effect on the dynamic tests results.

3.5. Dynamic load tests

After explosive loading, all the plates crushed into dozens of fragments larger than 1 mm, and their central part (contacting the detonator) turned into a fine pow-

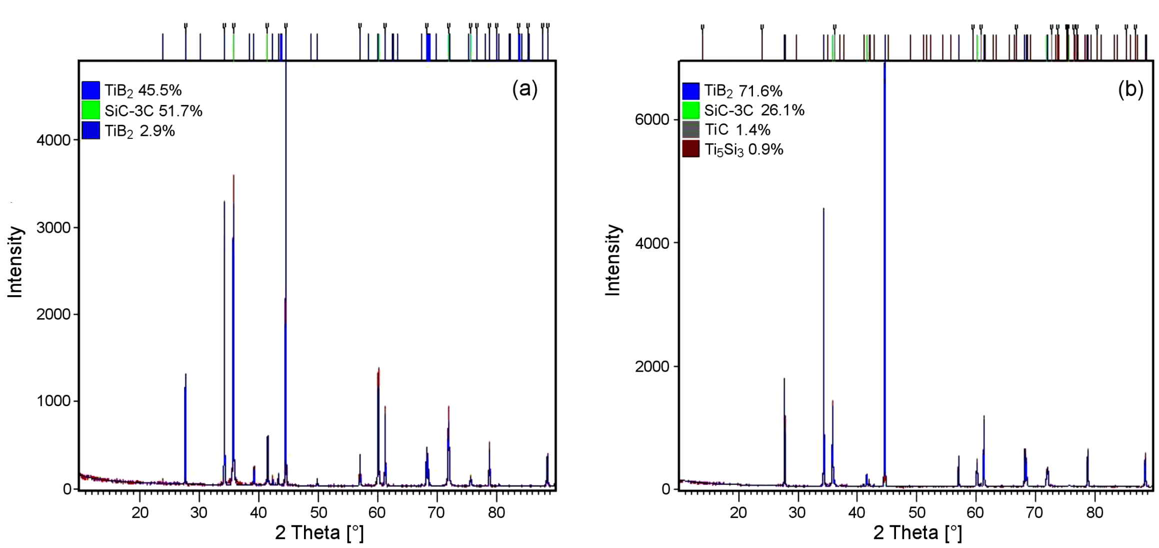

Figure 4. XRD patterns of the composites sintered at 1550 °C and 2.5 GPa: a) $B_4C/TiSi_2$-S and b) B_4C/Ti_5Si_3-S

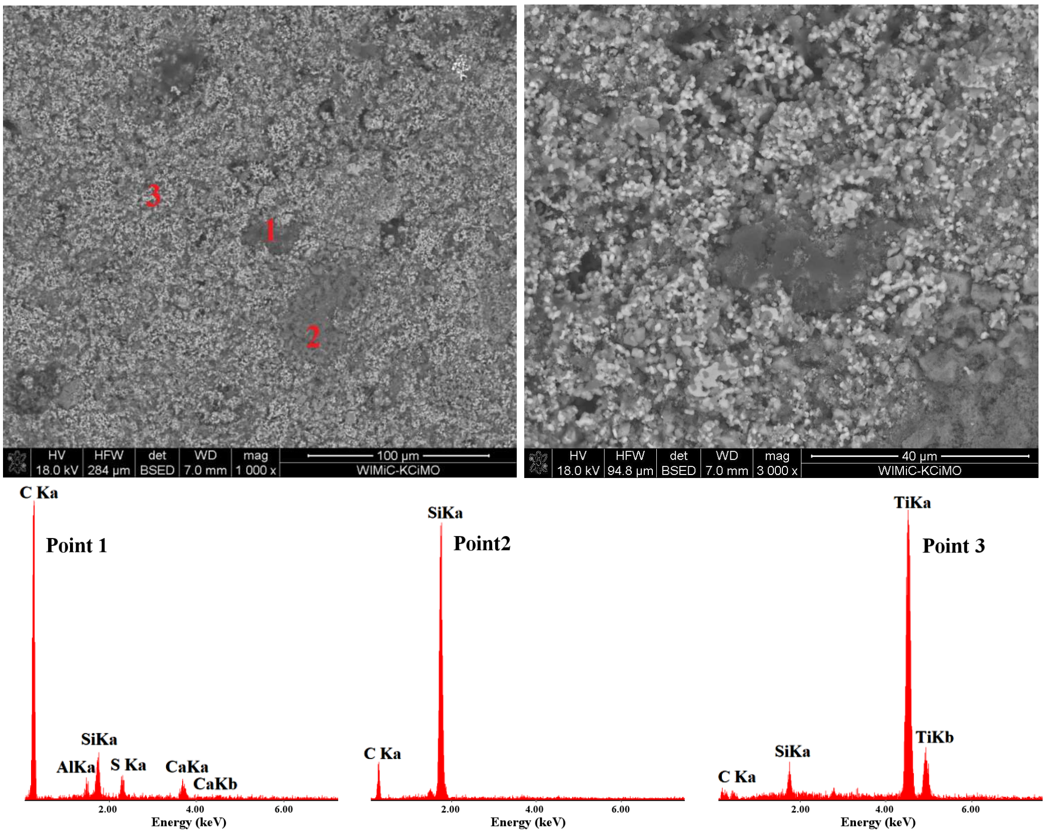

Figure 5. SEM images and EDS analyses of the sintered $B_4C/TiSi_2$-S ceramics

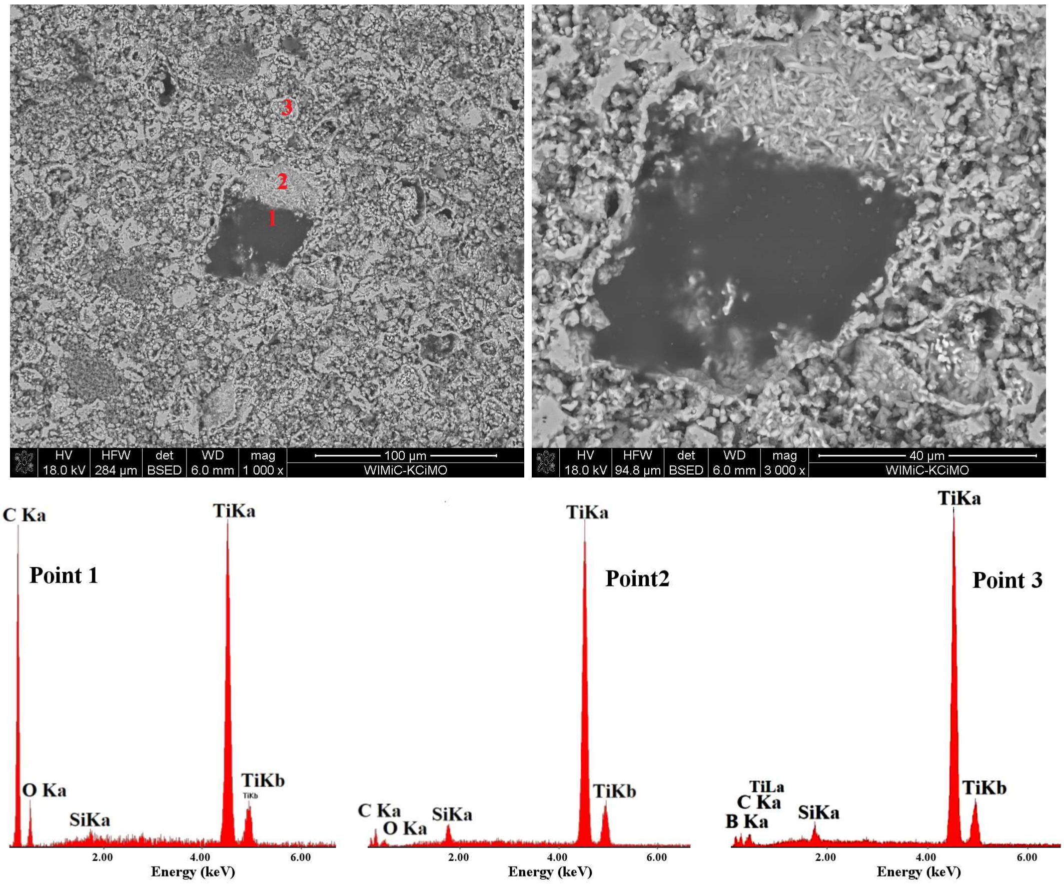

Figure 6. SEM images and EDS analyses of the sintered B_4C/Ti_5Si_3-S ceramics

Table 3. Pulverization level of the composites after dynamic load tests

Sintered sample	Mass of initial sample [g]	Mass of large fragments [g]	Pulverization level [%]
$B_4C/TiSi_2$-20	29.39	22.04	25
$B_4C/TiSi_2$-S	29.78	26.92	10


(a) (b)

Figure 7. Photographs of the chamber bottom after the explosion of the sintered samples a) $B_4C/TiSi_2$-20 and b) $B_4C/TiSi_2$-S

der in each case (Fig. 7). The larger sample fragments were collected and weighed. Since the initial mass of each sample and the mass of the larger sample fragments were known, the pulverization level of each studied system could be determined (Table 3).

The macroscale analysis of the post-mortem samples revealed their different behaviour, depending on the intermetallics proportions. For the test purpose, the fragmented parts measuring <1 mm were considered as powdered. The sintered sample $B_4C/TiSi_2$-20 containing 20 wt.% of intermetallic phase (Fig 7a) was more pulverized (the powder weight constituted more than 25% of the original sample). The sintered samples $B_4C/TiSi_2$-S got powdered to a much lesser extent, i.e. the powdered part mass was less than 10 wt.% (Fig 7b and Table 3).

3.6. Vickers analysis

Figure 8 shows that the hardness of the sintered composites increases with the increase of amount of intermetallic phase. The highest hardness values were obtained for the composites with stoichiometric content of $TiSi_2$ and Ti_5Si_3. The observed increase in hardness with increasing percentage of silicide additives in the freely sintered composites can be attributed to several factors. Firstly, the addition of silicides, particularly $TiSi_2$, enhances the densification process during sintering, leading to a reduction in porosity and improved overall mechanical properties. As the silicide content increases, it forms a more continuous network within the composite matrix, effectively strengthening the material's structure. This network acts as a barrier to the dislocation movement, thereby increasing the composite's resistance to deformation and, consequently, its hardness. The highest hardness values obtained for the composites with stoichiometric content of $TiSi_2$ can be explained by the optimal balance between the base material and the additive. At the stoichiometric ratio, $TiSi_2$ forms a well-defined crystalline structure that maximizes its strengthening effect on the composite. This optimal composition allows for the formation of strong intermetallic bonds between the silicide and the matrix material, further enhancing the composite's hardness. Additionally, the stoichiometric content ensures a uniform distribution of the silicide throughout the matrix, preventing the formation of weak spots or areas of excessive brittleness that could compromise the overall hardness of the composites.

Recent research on fabrication of B_4C-TiB_2-SiC composites and their use as armour for military vehicles provided important reference for this study [27]. Based on the literature, sintered materials with 20% of the intermetallic compound were classified as B_4C-TiB_2-SiC composites. Samples with a stoichiometric addition of an intermetallic compound ($TiSi_2$ or Ti_5Si_3) were classified as TiB_2-SiC composites due to the sole presence of these compounds in the sintered samples. Ballistic resistance tests have not been carried out for TiB_2-SiC composites; however, key parameters such as hardness and fracture toughness allow for estimating their ballistic resistance. Hardness values for TiB_2-SiC composites reported by Zhu *et al.* [25] and Liu *et al.* [26], as well as the direct correlation between hardness values and fracture toughness (K_{IC}) display good ballistic resistance for TiB_2-SiC composites. While the high hardness values of B_4C were confirmed by numerous studies beyond any doubt [11,29], B_4C-TiB_2-SiC composites are also

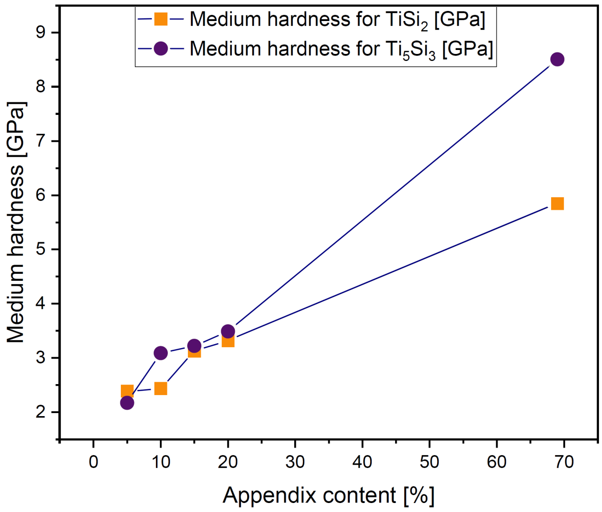

Figure 8. Correlation between average hardness and concentration of intermetallic phase for the $B_4C/TiSi_2$ and B_4C/Ti_5Si_3 composites

reported to be characterized by a high hardness value. Studies by Rodríguez-Rojas *et al.* [24] proved the feasibility of using this composite as body armour. Other studies, e.g. by Ming *et al.* [27], and Wang *et al.* [22,23], demonstrated that this material had high hardness and good mechanical properties. The tested TiB_2-SiC and B_4C-TiB_2-SiC composite samples gave similar results in terms of the key parameters for ballistic resistance. Thus, our results for the sintered samples with 20% intermetallic phases showed complementarity and compatibility with the results presented by Rodríguez-Rojas *et al.* [24]. Although the dynamic tests of the currently obtained systems ultimately did not confirm their usability as military vehicle armour, the results are promising enough, provided that the sintering process was properly optimized and all the quoted studies could find confirmation in an actual system.

IV. Conclusions

The reactively sintered TiB_2-SiC composites derived from boron carbide (B_4C) and intermetallics ($TiSi_2$ or Ti_5Si_3) were produced with either the 20 wt.% addition or stoichiometric amounts of intermetallics, which was the main goal of this study. XRD analyses of the stoichiometric proportion samples ($B_4C/TiSi_2$-S and B_4C/Ti_5Si_3-S) revealed a slight deviation from the theoretical assumptions. During the sintering process, the composite formation proceeded as assumed, but the sintering parameters require adjustments to achieve the full reaction of precursors. The leftover phases proved to be detrimental for the otherwise correct microstructure formation.

The performance of each sample and their partial pulverization values were assessed via the dynamic loading tests. For the samples containing 20% intermetallic compounds in the initial mixture, 25% of the sample was pulverized, In the case of the stoichiometric sample, the degree of pulverization was approximately 10%. Moreover, the pulverization level decreased with the increase of hardness, i.e. mass proportion of the intermetallic compounds. Based on those results, the two examined systems are currently insufficient for a vehicle armour material, regardless of the intermetallic type and its mass proportion. However, the composite fabrication with stoichiometric proportion of the precursor powders should be considered for future derivative research endeavours.

Acknowledgement: This research was supported by a grant from the National Center for Research and Development (LIDER XIII; Grant No. 0024/L-13/2022 (principal investigator: D. Kozień). The SEM-EDS investigations were supported by the program Excellence Initiative - Research University for the AGH University of Science and Technology, grant ID 1449 and co-funded by the Faculty of Materials Science and Ceramics AGH UST-University of Krakow, No. 16.16.160.557.

References

1. R.L. Woodward, "A simple one-dimensional approach to modelling ceramic composite armour defeat", *Int. J. Impact Eng.*, **9** [4] (1990) 455–474.
2. A. Krell, E. Strassburger, "Order of influences on the ballistic resistance of armor ceramics and single crystals", *Mater. Sci. Eng. A*, **597** (2014) 422–430.
3. Z. Shen, D. Hu, G. Yang, X. Han, "Ballistic reliability study on SiC/UHMWPE composite armor against armor-piercing bullet", *Compos. Struct.*, **213** (2019) 209–219.
4. P. Hu, Y. Cheng, P. Zhang, J. Liu, H. Yang, J. Chen, "A metal/UHMWPE/SiC multi-layered composite armor against ballistic impact of flat-nosed projectile", *Ceram. Int.*, **47** [16] (2021) 22497–22513.
5. L. Zheng, W. Wei, X. Dong, C. Zhang, Y. Zeng, C. Zhang, H. Huan, "Microscopic wear study of the sintered diamond trepanning drill during machining alumina armor ceramics", *Ceram. Int.*, **45** [3] (2019) 3986–3994.
6. A.C. Pereira, M.S. Oliveira, A.C. Pereira, L.F.C. Nascimento, J.R.G. Matheus, S.N. Monteiro, "Ballistic performance of multilayered armor with intermediate polyester composite reinforced with fique natural fabric and fibers", *J. Mater. Res. Technol.*, **8** [5] (2019) 4221–4226.
7. M. Aydin, M. Soydemir, "Ballistic protection performance of a free ceramic particle armor system: An experimental investigation", *Ceram. Int.*, **47** [8] (2021) 11628–11636.
8. P. Falkowski, R. Żurowski, "Shaping of alumina microbeads by drop-casting of the photopolymerizable suspension into silicone oil and UV curing", *J. Eur. Ceram. Soc.*, **42** [9] (2022) 3957–3967.
9. R. Żurowski, P. Falkowski, J. Zygmuntowicz, M. Szafran, "Rheological and technological aspects in designing the properties of shear thickening fluids", *Materials*, **14** [21] (2021) 6585.
10. M. Głuszek, R. Żurowski, M. Kubiś, T. Wiśniewski, M. Szafran, "Shear thickening behavior and thermal properties of nanofluids with graphite fillers", *Mater. Res. Express*, **6** [1] (2019) 15701.
11. A.B. Dresch, J. Venturini, S. Arcaro, O.R.K. Montedo, C.P. Bergmann, "Ballistic ceramics and analysis of their mechanical properties for armour applications: A review," *Ceram. Int.*, **47** [7] (2021) 8743–8761.
12. K. Dasgupta, "Role of carbon nanotubes in the ballistic properties of boron carbide/carbon nanotube/ultrahigh molecular weight polyethylene composite armor", *Ceram. Int.*, **46** [4] (2020) 4137–4141.
13. C. Cheng, K.M. Reddy, A. Hirata, T. Fujita, M. Chen, "Structure and mechanical properties of boron-rich boron carbides", *J. Eur. Ceram. Soc.*, **37** [15] (2017) 4514–4523.
14. W. Zhang, S. Yamashita, H. Kita, "Progress in pressureless sintering of boron carbide ceramics – a review", *Adv. Appl. Ceram.*, **118** [4] (2019) 222–239.
15. A. Gubernat, W. Pichór, D. Zientara, M.M. Bućko, Ł. Zych, D. Kozień, "Direct synthesis of fine boron carbide powders using expanded graphite", *Ceram. Int.*, **45** [17] (2019) 22104–22109.
16. D.Y. Kovalev, S.V. Konovalihin, "Boron carbide", pp. 42–44 in *Concise Encyclopedia of Self-Propagating High-Temperature Synthesis History, Theory, Technology, and Products*, Elsevier Inc., 2017.
17. J.L. Watts, H.J. Spratt, P.C. Talbot, J.A. Alarco, N.A. Raftery, I.D.R. Mackinnon, "Precision structural and phase analysis of boron carbide", *Ceram. Int.*, **46** [8]

(2020) 11033–11040.

18. D. Gosset, "Basic properties of boron carbide", pp. 539–553 in *Reference Module in Materials Science and Materials Engineering*, 2020.
19. S. Gao, X. Li, S. Wang, P. Xing, J. Kong, G. Yang, "A low cost, low energy, environmentally friendly process for producing high-purity boron carbide", *Ceram. Int.*, **45** [3] (2019) 3101–3110.
20. A. Chakraborti, A. Jay, O.H. Duparc, J. Sjakste, K. Béneut, N. Vast, Y. Le Godec, "Boron carbide under torsional deformation: Evidence of the formation of chain vacancies in the plastic regime", *Acta Mater.*, **226** (2022) 117553.
21. K. Xia, M. Ma, C. Liu, H. Gao, Q. Chen, J. He, J. Sun, H.T. Wang, Y. Tian, D. Xing, "Superhard and superconducting B_6C", *Mater. Today Phys.*, **3** (2017) 76–84.
22. Y. Wang, Q. Liu, B. Zhang, H. Zhang, Y. Jin, Z. Zhong, J. Ye, Y. Ren, F. Ye, W. Wang, "Microstructure and mechanical behaviour of transient liquid phase spark plasma sintered B_4C-SiC-TiB_2 composites from a B_4C-$TiSi_2$ system", *Ceram. Int.*, **47** [8] (2021) 10665–10671.
23. S. Wang, L. Li, S. Yan, Y. Deng, S. Gao, P. Xing, "Preparing B_4C-SiC-TiB_2 composites via reactive pressureless sintering with B_4C and $TiSi_2$ as raw materials", *J. Mater. Res. Technol.*, **9** [4] (2020) 8685–8696.
24. F. Rodríguez-Rojas, V. Zamora, F. Guiberteau, A.L. Ortiz, "Wear of the ultrahard B_4C-SiC-TiB_2 ceramic composite in unlubricated sliding contact with ceramic counterparts", *J. Eur. Ceram. Soc.*, **44** [10] (2024) 5555–5568.
25. M. Zhu, J. Chen, F.F. Li, C.C. Huang, H. Liu, X.J. Liu, Z.R. Huang, "Fabrication and characterization of SiC-TiB_2 composite ceramics used as infrared source material", *Ceram. Int.*, **49** [7] (2023) 11504–11512.
26. J. Liu, Y. Li, C. Cheng, W. Li, X. Qin, "Effect of temperature on the structure and mechanical properties of SiC-TiB_2 composite ceramics by solid-phase spark plasma sintering", *Ceram. Int.*, **48** [16] (2022) 23151–23158.
27. L. Ming, Q. Song, Z.T. Cheng, Z.K. Wang, C. Wu, "Protection mechanism of B_4C-TiB_2-SiC composite ceramic under ultra-high velocity impact", *Ceram. Int.*, **50** [13] (2024) 24045–24053.
28. S. Rzepa, L. Chlubny, T. Bucki, "The Ti-Si intermetallic phases synthesis by SHS method", pp. 1699–1704 in *Metal 2018 - 27th Int. Conf. Metall. Mater. Conf. Proc.*, Brno, Czech Republic, 2018.
29. F. Thévenot, "Boron carbide-A comprehensive review", *J. Eur. Ceram. Soc.*, **6** [4] (1990) 205–225.